Engineered neural tissue for peripheral nerve repair

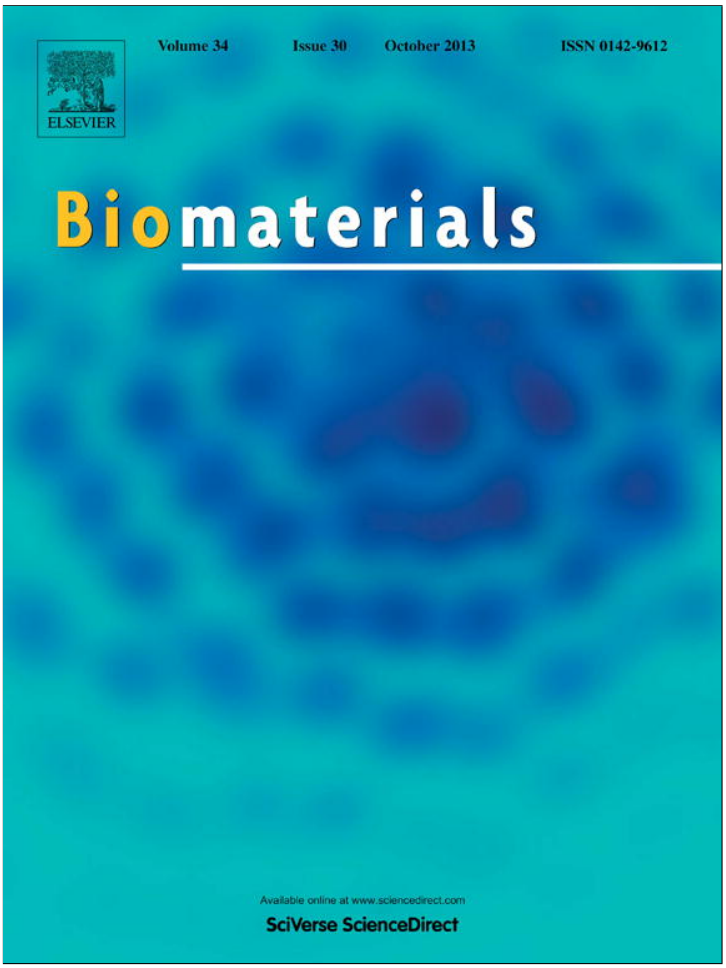

Biomaterials 34 (2013) 7335–7343

Contents lists available at SciVerse ScienceDirect

Biomaterials

journal homepage: www.elsevier.com/locate/biomaterials

Engineered neural tissue for peripheral nerve repair

Melanie Georgiou [a], Stephen C.J. Bunting [b], Heather A. Davies [a], Alison J. Loughlin [a], Jonathan P. Golding [a], James B. Phillips [a,*]

[a] The Open University, Walton Hall, Milton Keynes, MK7 6AA, UK
[b] University College London, Gower Street, London, WC1E 6BT, UK

ARTICLE INFO

Article history:
Received 7 May 2013
Accepted 12 June 2013
Available online 5 July 2013

Keywords:
Collagen
Schwann cell
Nerve guide
Nerve regeneration
Nerve tissue engineering
Hydrogel

ABSTRACT

A new combination of tissue engineering techniques provides a simple and effective method for building aligned cellular biomaterials. Self-alignment of Schwann cells within a tethered type-1 collagen matrix, followed by removal of interstitial fluid produces a stable tissue-like biomaterial that recreates the aligned cellular and extracellular matrix architecture associated with nerve grafts. Sheets of this engineered neural tissue supported and directed neuronal growth in a co-culture model, and initial *in vivo* tests showed that a device containing rods of rolled-up sheets could support neuronal growth during rat sciatic nerve repair (5 mm gap). Further testing of this device for repair of a critical-sized 15 mm gap showed that, at 8 weeks, engineered neural tissue had supported robust neuronal regeneration across the gap. This is, therefore, a useful new approach for generating anisotropic engineered tissues, and it can be used with Schwann cells to fabricate artificial neural tissue for peripheral nerve repair.

1. Introduction

Cellular and extracellular matrix (ECM) alignment is a common feature of biological tissues, with anisotropy being critical to function in many instances. Examples include the collagen fibres that orientate in response to force vectors and strengthen ECM in musculoskeletal tissues, and the tracts of aligned cells present within the nervous system. Furthermore, failure to recreate the aligned cellular and/or ECM architecture of native tissues is a limitation in clinical repair and reconstruction, with scarring and poor restoration of mechanical properties being common [1]. For this reason, much research into tissue engineering and biomaterials has focused on the development of anisotropic scaffolds to confer orientation on cells and to provide the mechanical properties associated with aligned ECM [2–4].

One tissue where the use of an aligned cellular substrate would potentially be of great benefit for clinical repair is peripheral nerve. Neuronal regeneration and functional recovery are problematic following nerve damage and, where there is a long (>3 cm) defect, the current clinical gold standard treatment involves using a nerve autograft which has limited availability and results in donor site morbidity [5]. Shorter gaps can be bridged using hollow conduits or primary repair, and decellularized allograft tissue is also available [6]. The nerve autograft contains aligned Schwann cells which support and guide regenerating neurites from the proximal to the distal side of the repair site, and recreating this anisotropic 3D cellular architecture is the focus of much research in the area of peripheral nerve repair [7–9].

A range of approaches are available for achieving anisotropic engineered tissues including the use of aligned fibres or channels, patterned surfaces, electrical and magnetic fields, mechanical loading and gradients of physical and chemical cues to organize engrafted and/or infiltrating cells. Promising recent approaches that have been used to generate anisotropic cellular substrates to support nerve regeneration in experimental nerve injury models include the use of Schwann cell-seeded aligned fibres made from synthetic polymers [10], Schwann cells seeded within longitudinally porous cross linked collagen scaffolds [11], differentiated adipose-derived stem cells seeded within decellularised nerve tissue [12], neural stem cells aligned on the luminal surface of patterned polylactide tubes [13], and strips of Schwann cell-seeded poly-3-hydroxybutyrate [14]. In all these cases the anisotropic structure was achieved through the use of a pre-aligned scaffold into which cells were seeded.

In an alternative approach to the conventional tissue engineering paradigm of using a structured scaffold to confer alignment on cells, we previously reported how self-alignment of Schwann cells could be achieved within a tethered collagen hydrogel [15].

* Corresponding author. Tel.: +44 (0)1908 858193.
E-mail address: james.b.phillips@open.ac.uk (J.B. Phillips).

0142-9612/$ – see front matter © 2013 Elsevier Ltd. All rights reserved.
http://dx.doi.org/10.1016/j.biomaterials.2013.06.025

This method exploited the natural ability of cells and ECM to form anisotropic 3D structures in response to endogenous (cell-generated) tension [3]. However, in the fully hydrated state such cellular hydrogels require continuous tethering to maintain their anisotropic structure, limiting their potential for use in clinical repair. Here we report an effective solution to this problem in which cellular self-alignment within a tethered collagen gel can be stabilized using plastic compression. Plastic compression involves the rapid removal of fluid from collagen gels [16] and has been adopted as a means to form tissue-like constructs for a range of repair scenarios [17–21]. By using this approach to stabilise self-aligned cell-seeded collagen gels we have developed a powerful new method to engineer anisotropic cellular biomaterials. The technology avoids the limitations associated with seeding cells into preformed scaffolds, uses native collagen rather than synthetic materials, and achieves a robust stable structure without the use of chemical cross-linking agents. In the study reported here we have focused on incorporating Schwann cells within the aligned material in order to form engineered neural tissue (EngNT) constructs that could potentially be used in peripheral nerve repair. It is clear however that, with suitable alternative cells, a similar approach could be adopted for the fabrication of a wide range of tissues.

Here we describe the methodology used to generate sheets of EngNT, and the characterisation of the cellular and extracellular structure of the material. Furthermore, the ability of EngNT to support and guide neuronal growth both *in vitro* and *in vivo* has been demonstrated.

2. Materials and methods

2.1. Fabrication of Schwann cell EngNT

Schwann cells were aligned within tethered collagen gels in rectangular stainless steel moulds according to methods described previously [3,22], before stabilisation by plastic compression as shown in Fig. 1. Schwann cells were from the rat Schwann cell line SCL 4.1/F7 (Health Protection Agency, UK) and were maintained in culture medium (Dulbecco's Modified Eagle's Medium (DMEM; Gibco) supplemented with penicillin and streptomycin (100U/ml and 100 mg/ml, respectively; Sigma) and 10% v/v foetal calf serum) in standard cell culture flasks. To prepare gels, 1 volume of 10× minimum essential medium (Sigma) was mixed with 8 volumes of type I rat tail collagen (2 mg/ml in 0.6% acetic acid; First Link, UK) and the mixture neutralised using sodium hydroxide before addition of 1 volume of Schwann cell suspension (final density 4×10^6 cells per ml of gel). One ml of this mixture was added to each mould at 4 °C and integrated with tethering mesh at opposite ends before setting at 37 °C for 10 min. Tethered gels were immersed in culture medium and incubated at 37 °C in a humidified incubator with 5% CO_2/95% air for 24 h to allow alignment to develop. Aligned cellular gels were stabilised by plastic compression, which has been described previously for unaligned cellular gels [3,16]. The plastic compression parameters used here were selected to ensure stabilisation was rapid, sufficient to retain cellular alignment in the absence of tethering, and caused minimal cell death. Aligned tethered gels were separated from the tethering mesh using a scalpel, placed on an absorbent paper pad and immediately compressed by loading the gel with 120 g for 1 min during which time fluid was absorbed by the paper pad underneath. The resulting sheets of EngNT were either transferred directly to 24-well plates for *in vitro* experiments, or rolled to form rods (approximately 200 μm diameter × 15 mm length), according to the spiral assembly protocol reported previously for unaligned plastic compressed gels [16] and maintained in culture medium for up to 24 h prior to *in vivo* experiments.

2.2. Scanning electron microscopy (SEM)

EngNT sheets were fixed in 4% paraformaldehyde in phosphate buffered saline (PBS) for 24 h at 4°C. These were post-fixed in 1% osmium tetroxide in phosphate buffer (PB), dehydrated through a graded series of acetone, infiltrated in liquid carbon dioxide in a critical point drying apparatus (Polaron, UK) before drying at the critical point of 31 °C. The dried samples were mounted on aluminium SEM stubs with double-sided carbon sticky tabs (Agar Scientific, UK), sputter coated with gold (Polaron sputter coater SC7640, UK) and examined in a Zeiss Supra 55 VP FEGSEM at 3 kV.

2.3. Transmission electron microscopy (TEM)

After excision and dissection of the middle of the repair constructs, samples were fixed in 4% paraformaldehyde in PBS for 24 h at 4 °C. These were post-fixed in 1% osmium tetroxide in PB, dehydrated through a graded series of acetone, flat-embedded in Epon epoxy resin and polymerized at 60 °C for 48 h. Semi-thin sections of 1 μm were cut using a glass knife on a UCT ultra microtome (Leica, UK), dried onto a poly-L-lysine coated microscope slides and stained with 1% toluidine blue with added 5% sodium borate. Ultrathin sections of 70 nm were cut with a diamond knife (Diatome, UK) and collected on copper slot grids with Pioloform/carbon support films. Sections were counter-stained with aqueous uranyl acetate and Reynolds' lead citrate before examination in a JEM 1400 TEM (JEOL, UK).

2.4. Assessment of EngNT in co-culture with neurons

All experimental procedures involving animals were conducted in accordance with the UK Animals (Scientific Procedures) Act (1986) and approved by the Open University animal ethics advisory group. Dissociated dorsal root ganglion (DRG) neurons were prepared from adult (200–300 g) Sprague Dawley rats. DRGs were incubated in collagenase (0.125%; Sigma) for 1.5 h at 37 °C then dissociated by trituration and washed twice with 20 ml of culture medium before being incubated for 18 h with cytosine arabinoside (0.01 mM) to deplete glia. The resulting cultures contained (>99%) neurons, which were seeded onto the surface of EngNT sheets, allowed to settle for 30 min, then constructs were immersed in culture medium at 37 °C in a humidified incubator with 5% CO_2/95% air. After 3 days the EngNT-neuron co-cultures were washed briefly in PBS and fixed in 4% paraformaldehyde at 4 °C for 24 h, then immunofluorescence staining was carried out as described previously for collagen gels [23,24], to detect βIII-tubulin positive neurons and S100 positive Schwann cells.

2.5. Surgical repair of rat sciatic nerve

Sprague Dawley rats were deeply anesthetised by inhalation of isoflurane (rats were from a colony that express a β-actin-green fluorescent protein reporter, though this marker was not used in the present study). The left sciatic nerve of each animal was exposed at mid-thigh and transected, then either a repair conduit or a nerve graft was positioned between the stumps to produce an inter-stump distance of 5 or 15 mm. Conduits or grafts were retained in place using three 10/0 epineurial sutures at each stump, then wounds were closed in layers and animals were allowed to recover for 4 or 8 weeks. Two experiments were conducted using the rat sciatic nerve model:

1. A 4-week experiment to assess two different ways to incorporate EngNT into a repair device ($n = 12$, 225–300 g rats) included three groups (4 rats in each) and used a 5 mm inter-stump distance with a NeuraWrap™ (Integra, US) sheath containing either (A) two EngNT rods, (B) two sheets of EngNT, and (C) empty conduit. NeuraWrap was cut to a length of 8 mm to allow a 1.5 mm overlap with each nerve stump, rods or sheets were positioned between the stumps, then the NeuraWrap was closed using 10/0 sutures along the seam. For group (B) the two EngNT sheets were used to line the central 5 mm section of the NeuraWrap prior to closure.
2. An 8-week experiment tested the ability of EngNT rods to support neuronal regeneration across a 15 mm inter-stump distance ($n = 15$, 250–500 g rats) and included three groups (5 rats in each). This used a NeuraWrap sheath (18 mm) for groups (A) two EngNT rods and (B) empty conduit, or a 15 mm nerve graft (C) taken from a littermate culled using CO_2 asphyxiation.

For each experiment, animals were culled following the recovery period using CO_2 asphyxiation and repaired nerves were excised under a dissecting microscope. For experiment 1, the proximal part of the repair device was embedded in OCT, frozen and sectioned transversely (10 μm sections) using a cryostat. For experiment 2, the middle of the repair device was removed and prepared for TEM, and cryostat sections were prepared as above from the proximal and distal parts of the device and the nerve stumps. The transverse sections that were used for analysis were from positions 1 mm into the proximal and distal stumps, or 1 mm into the proximal and distal parts of the repair site, measured from the end of the nerve stump in each case.

Sections were immunostained using mouse monoclonal anti-200 kDa neurofilament to detect axons (1:1000, Covance, Princeton, NJ) and visualised with DyLight 488 horse anti-mouse immunoglobulin secondary antibody (1:200, Vector Laboratories, Burlingame, CA). Primary antibody was incubated overnight at 4 °C and secondary antibody was incubated at room temperature for 45 min.

2.6. Microscopy and image analysis

Confocal microscopy (Leica SP5) was used in the assessment of Schwann cell alignment in EngNT and Schwann cell and neurite alignment and neurite growth in the EngNT-neuron co-cultures. Six equivalent fields were analysed per gel using a standardised sampling protocol. Images were captured using a ×40 oil immersion lens, z-stacks were 20 μm with a step size of 1 μm. Image analysis was conducted using Volocity™ software (Perkin Elmer, Waltham, MA) running automated 3D image analysis protocols to measure the angle of Schwann cell alignment and neurite alignment in each field. Neurite length per mm^2 was measured by tracing all

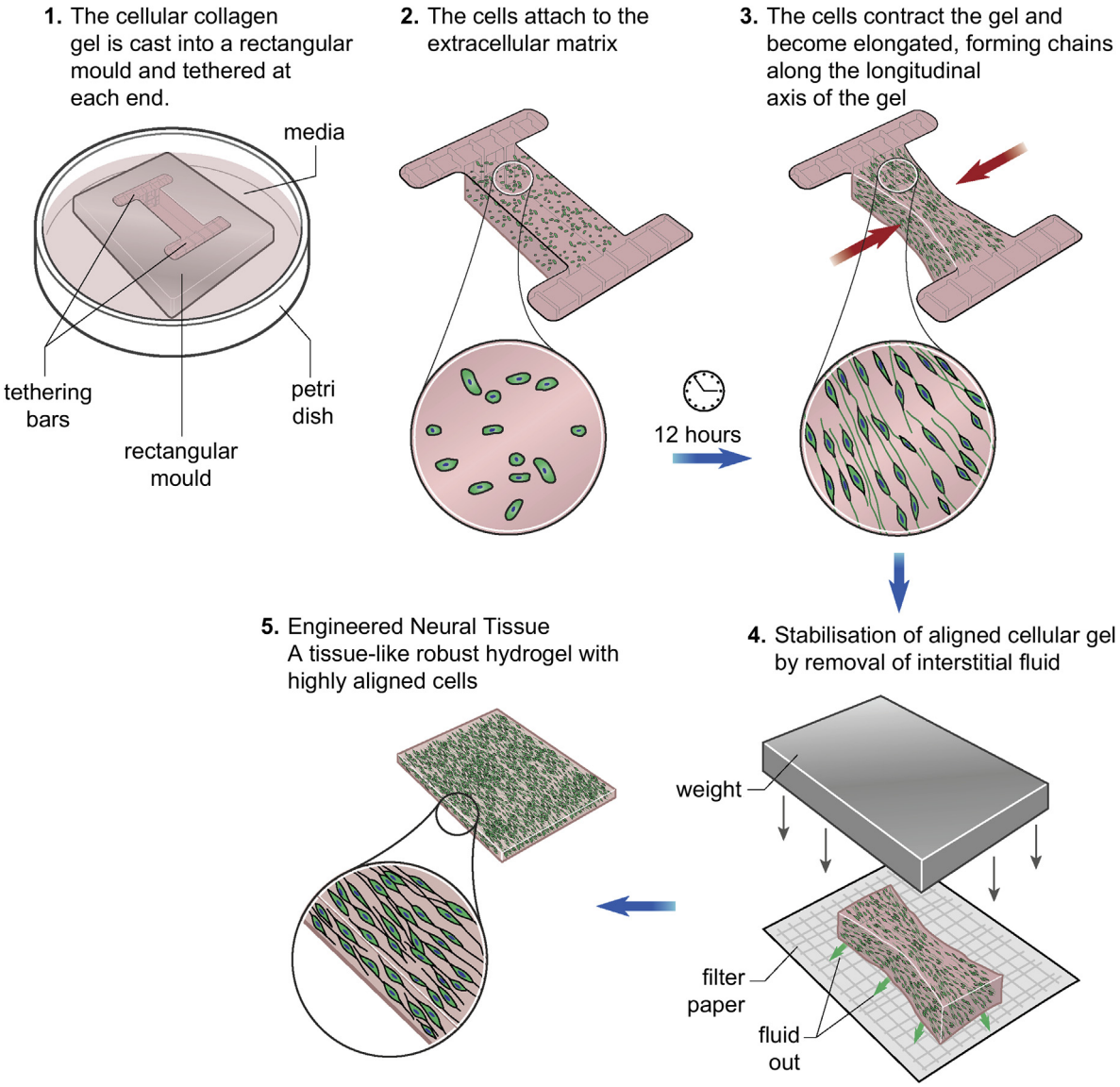

Fig. 1. Stages in the fabrication of EngNT. Schwann cells are set within a tethered collagen gel (1), the cells attach to the matrix (2) and self-align in parallel to the longitudinal axis (3), then the aligned cellular hydrogel is stabilised using plastic compression to remove interstitial fluid (4) and yield a robust engineered neural tissue (5).

of the βIII-tubulin-positive neurites within the confocal projection of each field using Openlab software (Improvision, UK).

Fluorescence microscopy (Olympus BX61) was used to capture images from the immunostained cryosections. To assess axonal growth, all of the neurofilament positive axons present in each transverse section were counted. In some cases the localization of each axon in relation to the EngNT material was assessed, in which case the EngNT was visualised using autofluorescence.

TEM ultrathin sections were imaged at a column magnification of ×2000 from the areas of greatest regeneration density as identified from the respective stained semi-thin sections. These images were coded for subsequent analyses, where Image J was used to measure axon diameter and fibre diameter, then myelin thickness and G-ratio were calculated where appropriate.

3. Results

3.1. Production of EngNT sheets

Fig. 1 shows the steps involved in generating sheets of EngNT through self-alignment of Schwann cells within a collagen gel followed by stabilisation using plastic compression. Preliminary studies established the Schwann cell-seeding density required to achieve optimal alignment, and live/dead staining using propidium iodide indicated that plastic compression resulted in no increase in cell death compared to fully hydrated gels (Supplementary Fig. 1). The sheets of EngNT were robust stable materials (40–60 μm thick). Confocal microscopy (Fig. 2a) showed that the EngNT contained elongated Schwann cells exhibiting a bipolar morphology (Fig. 2a(ii)), aligned parallel to the long axis of the material (Fig. 2b). Scanning electron microscopy revealed the corresponding alignment of collagen fibrils within the matrix following cellular self-alignment (Fig. 2c).

3.2. EngNT sheets support and guide neuronal growth in vitro

To determine the effectiveness of EngNT as a substrate for the support and guidance of neuronal growth, a co-culture was established by seeding primary rat sensory neurons onto the surface of EngNT sheets. Long straight neurites were detected growing in close contact with the Schwann cell processes in the material (Fig. 3a). The 3-dimensional orientation of the neurites was quantified and found to correspond closely to that of the Schwann cells (Fig. 3b), with 70% of neurites showing a deviation of less than 20° from the mean angle of Schwann cell alignment in each field.

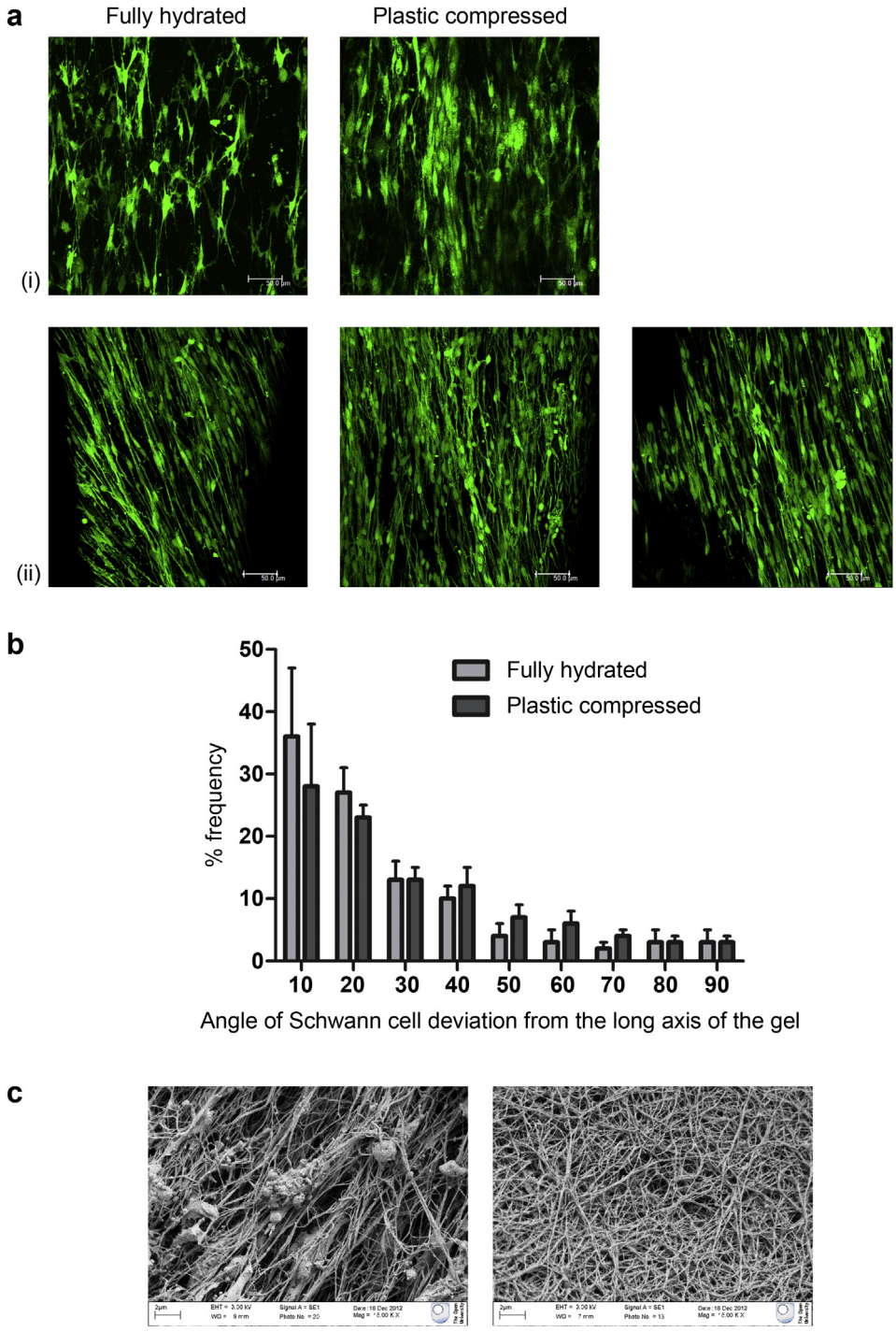

Fig. 2. Alignment of Schwann cells and collagen fibrils within EngNT. Confocal micrographs show highly aligned elongated Schwann cells (a); labelled with CellTracker to show live cells before and after plastic compression (i), and within EngNT using immunofluorescence (ii), z-distance 20 μm, step size 1 μm, scale bars 50 μm. Image analysis indicated that the cells were predominantly aligned with the longitudinal axis of the gel both before and after plastic compression (b); data are mean frequency of angle deviation (in 10° bins) ± SEM from 6 fields in each construct, $n = 3$ independent gels. Scanning EM (c) revealed the alignment of collagen fibrils in EngNT and their intimate association with the Schwann cells (i) in contrast to the random orientation of fibrils in equivalent acellular plastic compressed collagen material (ii), scale bars 2 μm.

The co-culture system was then used to investigate whether the efficacy of EngNT was dependent on the presence of living aligned Schwann cells, or whether a decellularised or an acellular version might also support neuronal regeneration. Control materials were either EngNT sheets that had been mostly decellularised by freeze-thaw (resulting in 96 ± 3% cell death) as described previously [25], or sheets formed by plastic compression of acellular collagen gels (made in the same way as EngNT but with no cells present and thus no alignment). The cumulative length of neurite growth within each 3D field was measured and Fig. 3c shows that while there was 56.8 ± 1.5 mm of neurite growth per mm^2 in the Schwann cell EngNT samples, there was relatively little neurite growth detected in equivalent fields from the decellularised and acellular materials (2.2 ± 0.3 and 1.2 ± 0.4 mm per mm^2, respectively), demonstrating

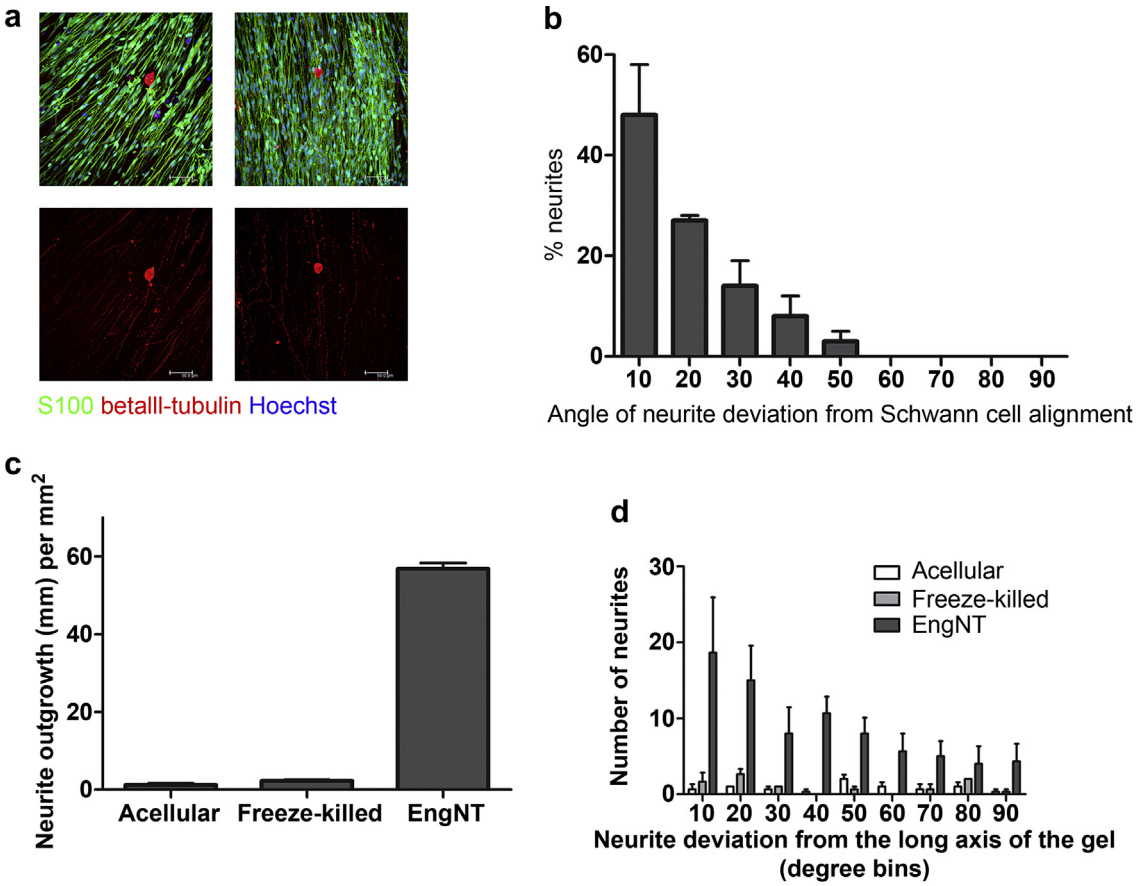

Fig. 3. EngNT containing live Schwann cells supports and guides the growth of neurites *in vitro*. Confocal micrographs (a) show Schwann cells (green) supporting aligned neurite growth (red) after 3 days in co-culture (z-dimension 20 μm, step size 1 μm). Three-dimensional image analysis was used to calculate the angle of deviation between the Schwann cell alignment and the neurite alignment in each of 4 fields per gel (b) and the frequency with which each angle of deviation occurred (in 10° bins) was determined (332 neurites were analysed). The total length of neurite staining detected per mm^2 was compared in EngNT and decellularised and acellular controls (c), 3 fields (total area 0.368 mm^2) were sampled in each gel. The angle of neurite growth was compared to the longitudinal axis of the construct in each case (d). Data are means ± SEM, $N = 3$ independent co-cultures. (For interpretation of the references to colour in this figure legend, the reader is referred to the web version of this article.)

the importance of the presence of live Schwann cells. Interestingly, there was more neurite growth detected with the decellularised material than the acellular material, and the growth that was present showed some orientation (Fig. 3d).

3.3. Implantation of devices containing sheets or rods of EngNT in short gap sciatic nerve injury model

Having demonstrated the ability of EngNT to support and guide neuronal regeneration *in vitro*, *in vivo* experiments were conducted to explore how EngNT could be delivered to a site of nerve damage and whether the orientated neuronal growth supported *in vitro* would occur in the more complex environment *in vivo*. Two potential approaches to delivering EngNT were compared using the 5 mm gap rat sciatic nerve model with Neurawrap™, a commercially available nerve conduit made from bovine collagen, as an outer sheath. One approach used two sheets of EngNT that had been rolled into two rods (Fig. 4a), whereas the other used two equivalent sheets of EngNT that were placed loosely within the Neurawrap™ sheath to form two concentric lining layers with longitudinal cellular alignment. Fig. 4b shows the distribution of neuronal regeneration at the mid-point of the conduits after 4 weeks. The cross sections were divided into zones and the number of axons per unit area in each zone was determined. Zone 1 was defined as the EngNT material, zone 2 was the region immediately adjacent to and extending 25 μm from the EngNT material and zone 3 was the remainder of the cross sectional area within the Neurawrap™ sheath (total internal cross sectional area of the device in each case was approximately 0.5 mm^2). An empty Neurawrap™ conduit group was included for comparison. The density of axonal growth within the empty Neurawrap™ tubes appeared to be lower than in zones 1 and 2 of the EngNT devices, but higher than the zone 3 regions of those devices, although these differences were not statistically significant. The rod device showed a significantly higher axon density within (zone 1) and adjacent to (zone 2) the EngNT compared to the surrounding area (zone 3), whereas the sheet device showed the same trend but this was less marked. Both designs confirmed the ability of EngNT to support dense neuronal growth, both within the material and within 25 μm of its surface.

3.4. EngNT supports neuronal regeneration across a 15 mm gap in vivo

To test the ability of EngNT to support neuronal regeneration in a clinically more relevant model, rods of EngNT were packed within Neurawrap™ to form an implantable device and used to repair a critical-sized defect of a 15 mm gap in the rat sciatic nerve (Supplementary Fig. 2 shows that in this model there was little regeneration within an empty conduit compared to a nerve graft). The EngNT devices were compared to empty Neurawrap™ tubes

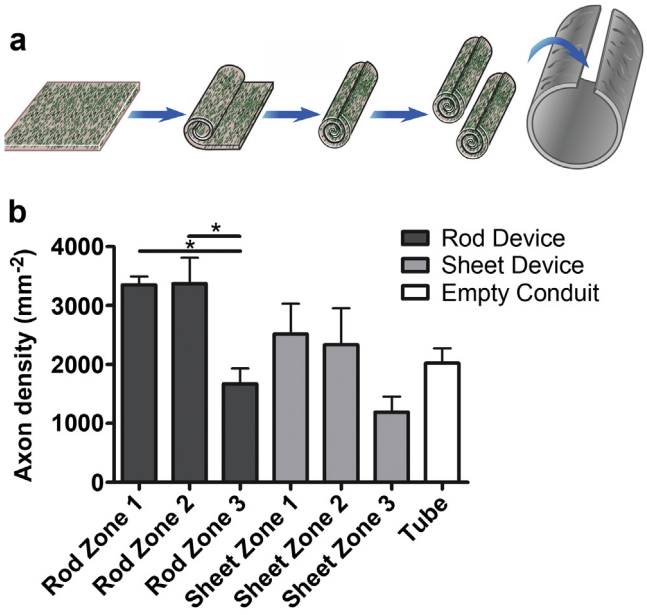

Fig. 4. Comparison between the inclusion of rods and sheets of EngNT within conduits *in vivo*. Flat sheets of EngNT were compared to rods, that were made by rolling the sheets, as an approach to delivery within a repair device (a). The different device designs were compared after 4 weeks recovery in a 5 mm rat sciatic nerve gap model, in terms of the distribution of regeneration within and around the EngNT in cross sections (b). One-way ANOVA with Tukey's post-test was used to compare three zones within each device group – the EngNT (zone 1), a region 25 μm from the EngNT surface (zone 2) and the remaining area within the conduit (zone 3) (*$P < 0.05$). An empty conduit was also included. *T*-tests were performed to compare the equivalent zone between each of the two device designs (no significant differences). Data are means ± SEM, $n = 4$.

and to grafts taken from the sciatic nerves of littermates to simulate the clinical gold standard autograft. The extent of neuronal regeneration across a 15 mm gap in the rat sciatic nerve was compared in these three surgical treatment groups, with assessment after 8 weeks of recovery.

Transverse sections were taken from the middle of the repair site and prepared for TEM. Fig. 5a shows 1 μm thick semi-thin resin sections stained with toluidine blue to reveal the extent of regenerated nerve tissue in each group. Dense neural tissue can be observed throughout the nerve graft and EngNT groups, with smaller patches of neural tissue present in the empty Neurawrap™ group. Fig. 5b shows representative transmission electron micrographs that reveal the detailed ultrastructure of the regenerated nerve tissue at the repair site. Because patches of regeneration were sparse within the empty conduits, analysis of nerve fibres was performed by selecting the areas of highest tissue density rather than sampling randomly, so that a representative population of regenerating fibres could be obtained from the empty conduit controls. Myelinated and unmyelinated nerve fibres were present in all groups and these were further classified according to axon diameter into 4 groups (<1 μm, 1–6 μm, 6–12 μm and 12–20 μm). The distribution of diameters for the myelinated (Fig. 5c(i)) and unmyelinated (Fig. 5c(ii)) nerve fibres shows that the population of neuronal fibre types that EngNT supported was equivalent to that present in the nerve graft. There was no significant difference between the EngNT device, the nerve graft and the empty conduit in terms of the populations of neuronal fibre types that had regenerated after 8 weeks. Most of the myelinated axons were in the 1–6 μm group, with a smaller proportion in the <1 μm group and very few larger diameter axons present. The unmyelinated axons were mainly <1 μm in diameter with some 1–6 μm and none with larger diameters.

The myelinated nerve fibres were explored further to assess the nature of the myelination present in each repair group (Fig. 5d). For each myelinated fibre, the diameter of the axon and the diameter of the fibre (axon + myelin sheath) was determined, allowing the thickness of the myelin and the G-ratio (axon diameter/fibre diameter) to be calculated. Both the axon diameter and fibre diameter were significantly lower in the empty conduit group compared to the nerve graft group, whereas there was no significant difference between the EngNT group and the nerve graft group (Fig. 5d(i, ii)). The myelin was thicker in the nerve graft group than both the EngNT and empty conduit group, and there was no significant difference in G-ratio between the three groups (Fig. 5 d(iii, iv)).

In addition to characterising the nature and distribution of neuronal regeneration and myelination at the mid-point of the EngNT conduit, further analyses were conducted using transverse sections through the proximal and distal ends of the repair site and the distal stump to investigate the effectiveness of EngNT in supporting regeneration across the 15 mm gap during the 8 week experiment (Fig. 6a). There was no significant difference between the number of axons that were present in the proximal part of the EngNT conduit and the empty conduit, however there were approximately twice as many axons in the proximal part of the nerve grafts (4584 ± 231) than the conduits. To assess regeneration across the gap in the two conduit groups, the number of axons in the distal end of the conduit and the distal stump was expressed as a percentage of the number of axons detected in the proximal part of the conduit. There was no significant difference between the number of neurites detected in the proximal conduit and distal conduit of the EngNT devices (repeated measures ANOVA), although there was a trend towards there being (~30%) fewer neurites in the distal device than had entered the proximal part of the device (Fig. 6b). In contrast, there were significantly (~90%) fewer neurites in the distal part of the empty conduit than entered the proximal part of the empty conduit.

4. Discussion

The process reported here resulted in sheets of robust cellular material containing highly aligned columns of Schwann cells within an aligned collagen matrix. This mimetic neural tissue therefore incorporated key cellular features known to contribute to the nerve repair process (elongated aligned Schwann cells with pro-regenerative phenotype), supported within a matrix that resembled natural endoneurium (aligned fibrils of type I collagen). In contrast to many other tissue engineering approaches (for recent reviews see Refs. [8,9,26]), the formation of EngNT involves simply directing natural cell–matrix interactions in order to achieve a highly organised anisotropic structure, which is then stabilised by gentle removal of excess fluid to leave a final tissue-like construct. This avoids the need to manufacture elaborate porous or fibrillar scaffolds with surface modification to support cell attachment, and cells are distributed throughout the material from the outset thus avoiding the need for a cell-seeding step. The cell matrix interactions that shape the anisotropic structure occur naturally in tissue development and remodelling, avoiding the complex spatial and mechanical cues that arise when cells are forced to grow on stiff surfaces (such as within pores and channels or on the surfaces of fibres) [3,27]. Furthermore, the use of plastic compression to stabilise the material avoids the need for chemical cross-linking agents and retains the protein in a native state suitable for integration with host tissue. Finally, the two-stage process of self-alignment and plastic compression is appropriate for scale-up and automation and can be used in combination with a range of cell types and hydrogel matrices, providing a versatile approach for

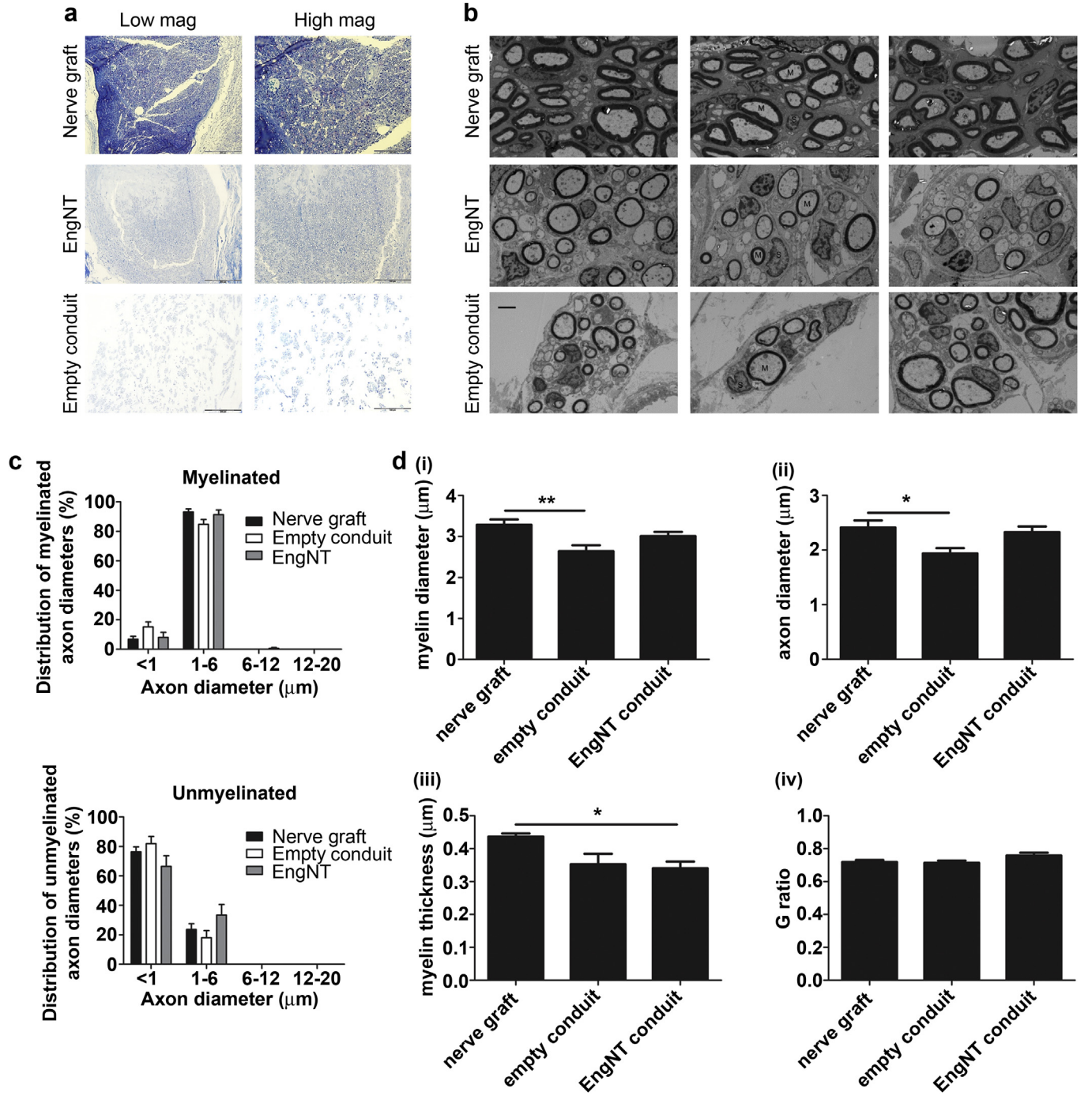

Fig. 5. EngNT supports neuronal regeneration in a long gap rat sciatic nerve injury model. Following 8 weeks recovery post-surgery, the mid-points of the 15 mm conduits or nerve grafts were examined. Representative semi-thin sections stained with toluidine blue (a) show the differences in density of regenerated neural tissue between the three groups at low and high magnification (scale bars 200 μm and 100 μm respectively). Areas with the highest density in each case were sampled for TEM (b) (M = Myelinated axon, S = Schwann cell nucleus, scale bar 2 μm), with 10 fields selected from the densest regions of each corresponding ultrathin section used to assess axonal diameter (c) and myelination (d). Data are means ± SEM, $n = 5$, $^{*}P < 0.05$, $^{**}P < 0.01$, one-way ANOVA with Tukey's post-test.

manufacturing aligned cellular materials that could be used in clinical and commercial settings.

The *in vitro* experiments demonstrated the ability of sheets of Schwann cell EngNT to support robust neuronal regeneration from adult rat DRG neurons. This only occurred when living Schwann cells were present and is in agreement with other studies using *in vitro* assays to show the pro-regenerative effect of Schwann cells on neurons in culture [28,29]. The neuronal growth was highly aligned parallel to the Schwann cell orientation, showing the ability of EngNT to provide guidance, and corresponding with previous reports that used orientated Schwann cell monolayer cultures or synthetic replicas of aligned Schwann cell topography to direct neuronal growth *in vitro* [30–32]. Neuronal cell bodies were seeded onto the surface of EngNT sheets, but confocal microscopy revealed that neurite growth occurred throughout the material and was not restricted to the top surface. The neurites were in close contact with

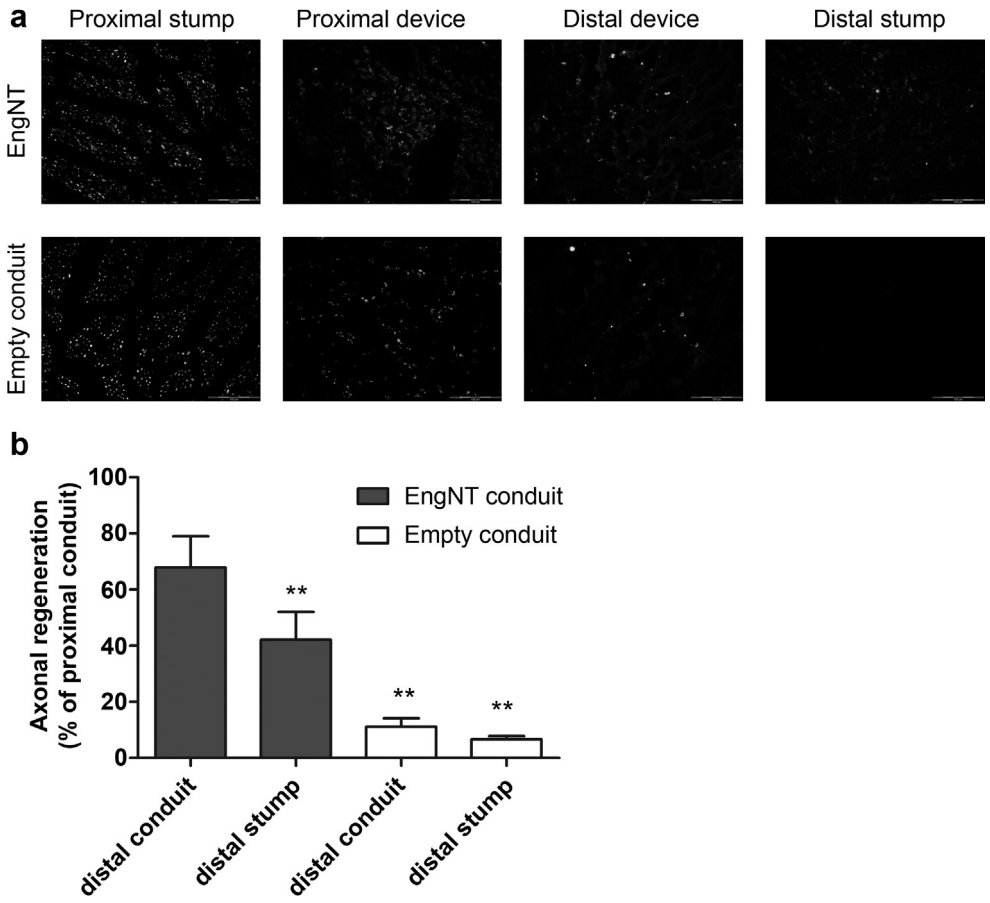

Fig. 6. EngNT supports neuronal regeneration through a 15 mm conduit and into the distal nerve stump. Transverse sections were taken at different positions within NeuraWrap conduits containing EngNT and empty NeuraWrap controls, and in the distal nerve stumps, and regenerated axons were detected using neurofilament immunoreactivity (a). The ability of each conduit to support neuronal growth was assessed by comparing the number of axons detected at the proximal end to those detected at the distal end and in the distal stump (b). Data are means ± SEM showing the number of axons at each position as a % of those present in the proximal device (proximal device axon counts were 2313 ± 260 for EngNT and 2059 ± 446 for empty conduit). There was no significant difference in the number of axons present in the distal compared to the proximal EngNT conduit (**$P < 0.01$, repeated measures ANOVA with Dunnett's post-test comparing distal regions to proximal device in each case).

the Schwann cells and the way they appeared to extend along the chains of glia was reminiscent of neuronal behaviour *in vivo* during regeneration [33].

The potential ability of EngNT to promote neuronal regeneration *in vivo* was investigated using a rat sciatic nerve injury model (for a review of common animal models for peripheral nerve repair see Ref. [34]). An experiment using a short (5 mm) gap model with a short recovery period (4 weeks) was used to explore the effect of delivering EngNT to a repair site. Neuronal regeneration resembled the pattern observed *in vitro*, with neurons growing within and on the surface of the EngNT material in preference to other regions of the conduit lumen. There are potentially many different ways to organize EngNT within a conduit and two possibilities (rods and sheets) were compared in the short gap model. EngNT rolled to form rods was easier to handle than sheets (which would be a consideration for clinical translation) and, despite the increased EngNT volume and surface area present in the sheet constructs after 4 weeks, there was no associated increase in regeneration compared to the compact rods. Another advantage of rolling EngNT into rods is that they are more likely than sheets to remain longitudinally aligned *in vivo*, which combines the cell-level anisotropy provided by the material with 'z' direction guidance across the cross-section of the scaffold [35]. It would be interesting to examine other ways to organise EngNT within conduits in future experiments in order to optimise regeneration support and ease of assembly.

Based on observations from the short gap experiment, EngNT rolled to form rods was selected for a more detailed investigation of regeneration support *in vivo* using a longer gap. The 15 mm gap rat sciatic nerve model provides a more challenging environment for testing repair devices since it represents a critical sized defect [8,34] in which an empty conduit performs poorly compared to a nerve graft (Supplementary Fig. 2). An 8 week experiment in a gap of this length was used to assess the support that could potentially be provided by EngNT to neurons regenerating within a conduit. At the mid-point of the repair there was considerably more tissue present in the EngNT group compared to the empty conduits, and electron microscopy revealed that the tissue associated with the EngNT contained densely packed nerve fibres associated with Schwann cells. Detailed analysis of the fibre types (based on diameter and presence of myelination) showed similar populations in all repair groups, with mainly smaller diameter fibres being present, in common with previous studies showing a shift towards smaller fibres in regenerating nerves compared to undamaged tissue [36].

Nerve repair materials need to support neuronal regeneration from proximal to distal stump, so the ability of EngNT to perform this role was investigated by assessing cross sections through the proximal and distal parts of the conduit as well as the stumps. Approximately half as many neurites entered the EngNT conduit compared to the nerve graft, possibly because the two EngNT rods

only occupied a fraction of the lumen (rod cross-sectional area was 12.9 ± 2.2% of the lumen cross sectional area), so did not form an interface with the complete cross-section of the proximal stump. Future work should therefore include optimizing the quantity and arrangement of EngNT in order to maximize proximal ingrowth. Of the neurites present in the proximal part of the conduit, approximately 70% successfully reached the distal conduit and approximately two thirds of these entered the distal stump. In contrast, only 10% of the neurites present at the proximal end regenerated through the empty conduit.

The *in vivo* experiments demonstrated that there is potential for EngNT to be used within a nerve repair conduit in order to promote neuronal regeneration across a critical sized defect. Further work will be required to establish the best design for an EngNT-based conduit that could be tested in terms of efficacy in a preclinical model, allowing functional outcomes over longer recovery periods to be assessed. This will require first optimising the amount and organisation of EngNT and incorporating a clinically appropriate source of Schwann cells [9,37].

5. Conclusions

The technology reported here offers a simple, rapid and effective method for the manufacture of aligned cellular biomaterials and could be applied to a broad range of tissue engineering applications. We have demonstrated the ability of the technique to be applied to the assembly of EngNT that has potential to be used in the construction of nerve repair conduits.

Acknowledgements

The authors are grateful to Biomedical Research Unit staff for post-surgical animal care, Francis Colyer for SEM sample preparation, Gordon Imlach for operation of the SEM and Julia Barkans for microscopy support.

Appendix A. Supplementary data

Supplementary data related to this article can be found at http://dx.doi.org/10.1016/j.biomaterials.2013.06.025.

References

[1] Brown RA, Phillips JB. Cell responses to biomimetic protein scaffolds used in tissue repair and engineering. Int Rev Cytol 2007;262:75–150.
[2] Park H, Cannizzaro C, Vunjak-Novakovic G, Langer R, Vacanti CA, Farokhzad OC. Nanofabrication and microfabrication of functional materials for tissue engineering. Tissue Eng 2007;13:1867–77.
[3] Phillips JB, Brown R. Micro-structured materials and mechanical cues in 3D collagen gels. Methods Mol Biol 2011;695:183–96.
[4] Lim JY, Donahue HJ. Cell sensing and response to micro- and nanostructured surfaces produced by chemical and topographic patterning. Tissue Eng 2007;13:1879–91.
[5] Deumens R, Bozkurt A, Meek MF, Marcus MA, Joosten EA, Weis J, et al. Repairing injured peripheral nerves: bridging the gap. Prog Neurobiol 2010;92:245–76.
[6] Szynkaruk M, Kemp SW, Wood MD, Gordon T, Borschel GH. Experimental and clinical evidence for use of decellularized nerve allografts in peripheral nerve gap reconstruction. Tissue Eng Part B Rev 2012.
[7] Pabari A, Yang SY, Mosahebi A, Seifalian AM. Recent advances in artificial nerve conduit design: strategies for the delivery of luminal fillers. J Control Release 2011;156:2–10.
[8] Nectow AR, Marra KG, Kaplan DL. Biomaterials for the development of peripheral nerve guidance conduits. Tissue Eng Part B Rev 2012;18:40–50.
[9] Daly W, Yao L, Zeugolis D, Windebank A, Pandit A. A biomaterials approach to peripheral nerve regeneration: bridging the peripheral nerve gap and enhancing functional recovery. J R Soc Interface 2012;9:202–21.
[10] Lietz M, Dreesmann L, Hoss M, Oberhoffner S, Schlosshauer B. Neuro tissue engineering of glial nerve guides and the impact of different cell types. Biomaterials 2006;27:1425–36.
[11] Bozkurt A, Deumens R, Beckmann C, Olde Damink L, Schugner F, Heschel I, et al. In vitro cell alignment obtained with a Schwann cell enriched microstructured nerve guide with longitudinal guidance channels. Biomaterials 2009;30:169–79.
[12] Zhang Y, Luo H, Zhang Z, Lu Y, Huang X, Yang L, et al. A nerve graft constructed with xenogeneic acellular nerve matrix and autologous adipose-derived mesenchymal stem cells. Biomaterials 2010;31:5312–24.
[13] Hsu SH, Su CH, Chiu IM. A novel approach to align adult neural stem cells on micropatterned conduits for peripheral nerve regeneration: a feasibility study. Artif Organs 2009;33:26–35.
[14] Kalbermatten DF, Erba P, Mahay D, Wiberg M, Pierer G, Terenghi G. Schwann cell strip for peripheral nerve repair. J Hand Surg Eur Vol 2008;33:587–94.
[15] Phillips JB, Bunting SC, Hall SM, Brown RA. Neural tissue engineering: a self-organizing collagen guidance conduit. Tissue Eng 2005;11:1611–7.
[16] Brown RA, Wiseman M, Chuo CB, Cheema U, Nazhat SN. Ultrarapid engineering of biomimetic materials and tissues: fabrication of nano- and microstructures by plastic compression. Adv Funct Mater 2005;15:1762–70.
[17] Levis HJ, Brown RA, Daniels JT. Plastic compressed collagen as a biomimetic substrate for human limbal epithelial cell culture. Biomaterials 2010;31:7726–37.
[18] Braziulis E, Diezi M, Biedermann T, Pontiggia L, Schmucki M, Hartmann-Fritsch F, et al. Modified plastic compression of collagen hydrogels provides an ideal matrix for clinically applicable skin substitutes. Tissue Eng Part C Methods 2012;18:464–74.
[19] Micol LA, Ananta M, Engelhardt EM, Mudera VC, Brown RA, Hubbell JA, et al. High-density collagen gel tubes as a matrix for primary human bladder smooth muscle cells. Biomaterials 2011;32:1543–8.
[20] Bitar M, Salih V, Brown RA, Nazhat SN. Effect of multiple unconfined compression on cellular dense collagen scaffolds for bone tissue engineering. J Mater Sci Mater Med 2007;18:237–44.
[21] East E, de Oliveira DB, Golding JP, Phillips JB. Alignment of astrocytes increases neuronal growth in three-dimensional collagen gels and is maintained following plastic compression to form a spinal cord repair conduit. Tissue Eng Part A 2010;16:3173–84.
[22] Brown RA, Phillips JB. Self-aligning tissue growth guide. 2004; Patent number WO/2004/087231.
[23] Wright KE, Liniker E, Loizidou M, Moore C, Macrobert AJ, Phillips JB. Peripheral neural cell sensitivity to mTHPC-mediated photodynamic therapy in a 3D in vitro model. Br J Cancer 2009;101:658–65.
[24] East E, Golding JP, Phillips JB. A versatile 3D culture model facilitates monitoring of astrocytes undergoing reactive gliosis. J Tissue Eng Regen Med 2009;3:634–46.
[25] Hadjipanayi E, Cheema U, Mudera V, Deng D, Liu W, Brown RA. First implantable device for hypoxia-mediated angiogenic induction. J Control Release 2011;153:217–24.
[26] Bell JH, Haycock JW. Next generation nerve guides: materials, fabrication, growth factors, and cell delivery. Tissue Eng Part B Rev 2012;18:116–28.
[27] Grinnell F. Fibroblast biology in three-dimensional collagen matrices. Trends Cell Biol 2003;13:264–9.
[28] Armstrong SJ, Wiberg M, Terenghi G, Kingham PJ. ECM molecules mediate both Schwann cell proliferation and activation to enhance neurite outgrowth. Tissue Eng 2007;13:2863–70.
[29] Kingham PJ, Kalbermatten DF, Mahay D, Armstrong SJ, Wiberg M, Terenghi G. Adipose-derived stem cells differentiate into a Schwann cell phenotype and promote neurite outgrowth in vitro. Exp Neurol 2007;207:267–74.
[30] Thompson DM, Buettner HM. Neurite outgrowth is directed by schwann cell alignment in the absence of other guidance cues. Ann Biomed Eng 2006;34:161–8.
[31] Richardson JA, Rementer CW, Bruder JM, Hoffman-Kim D. Guidance of dorsal root ganglion neurites and Schwann cells by isolated Schwann cell topography on poly(dimethyl siloxane) conduits and films. J Neural Eng 2011;8:046015.
[32] Seggio AM, Narayanaswamy A, Roysam B, Thompson DM. Self-aligned Schwann cell monolayers demonstrate an inherent ability to direct neurite outgrowth. J Neural Eng 2010;7:046001.
[33] Ribeiro-Resende VT, Koenig B, Nichterwitz S, Oberhoffner S, Schlosshauer B. Strategies for inducing the formation of bands of Bungner in peripheral nerve regeneration. Biomaterials 2009;30:5251–9.
[34] Angius D, Wang H, Spinner RJ, Gutierrez-Cotto Y, Yaszemski MJ, Windebank AJ. A systematic review of animal models used to study nerve regeneration in tissue-engineered scaffolds. Biomaterials 2012;33:8034–9.
[35] Bellamkonda RV. Peripheral nerve regeneration: an opinion on channels, scaffolds and anisotropy. Biomaterials 2006;27:3515–8.
[36] Ikeda M, Oka Y. The relationship between nerve conduction velocity and fiber morphology during peripheral nerve regeneration. Brain Behav 2012;2:382–90.
[37] Mantovani C, Terenghi G, Shawcross SG. Isolation of adult stem cells and their differentiation to schwann cells. Methods Mol Biol 2012;916:47–57.